Short communication

A novel method to fabricate nonstoichiometric LiFePO$_4$/C core–shell composites

Qi Fan, YueFeng Tang*, YanFeng Chen*

Department of Materials Science and Engineering, College of Engineering and Applied Sciences, National Laboratory of Solid State Microstructures, Nanjing University, Nanjing 210093, People's Republic of China

ARTICLE INFO

ABSTRACT

The nonstoichiometric LiFePO$_4$/C core–shell composites (as microscale LiFePO$_4$ cores coated with 3–5 nm thin carbon shells) are synthesized by a novel solid-state reaction method. All samples show outstanding coulombic efficiency (about 100%) and good battery cyclability, along with high tap density (>1.70 g cm^{-3}). On this basis, the electrochemical properties of two different core–shell composites as Li$_{1.02}$Fe$_{0.99}$PO$_4$/C and Li$_{0.98}$Fe$_{1.01}$PO$_4$/C are compared. The results show that the rate performance of Li$_{1.02}$Fe$_{0.99}$PO$_4$/C is obviously better than the rate performance of Li$_{0.98}$Fe$_{1.01}$PO$_4$/C.

1. Introduction

As the large demands of strong hybrid, plug-in hybrid and especially battery electric vehicles in today's society, the requirement for improved power sources is continuing to increase [1]. Lithium ion battery has a bright future as one of the new power source technologies for its superior performance. But the global lithium-ion battery industry is far from developing an electric energy storage component suitable in both energy and power that will satisfy the demands of high power application, especially battery electric and hybrid vehicles. LiFePO$_4$ belongs to a new generation cathode material for lithium ion batteries. This material is regarded as the best candidate cathode material for battery-using of electric or hybrid vehicles as its advantages of non-toxicity, high thermal stability, low cost, good cycling performance [2–5]. However, the pure LiFePO$_4$ material has very poor rate performance because of its both low electronic and ionic conductivity [2–6]. Another impediment restricts the practical application of this material is its low tap density which leads a low volumetric specific capacity and that prevents us to achieve a high-energy-density lithium electrode [7,8].

Several strategies have been developed to enhance the electrochemical performance of LiFePO$_4$, including the design of nonstoichiometric compositions or core–shell structure with partially-graphitic carbon layer to improve the electron conductivity [2,5,9–14]. The typical methods to fabricate LiFePO$_4$/C core–shell structure are sol–gel, hydrothermal, etc. [9,11,13,15]. These methods may bring a great weight of carbon into the samples

in the synthesis process which decreases the tap density of the material. A more serious problem is that too thick carbon–shell on the surface of LiFePO$_4$ particles may hinder the Li$^+$ diffusion through the cathode/electrolyte interface which is very important for Li$^+$ transport in the charge/discharge process. A certain work have been done by Amine's group to solve this problem is using carbon deposition although this method cannot form the homogenous and continuous carbon-coating on the LiFePO$_4$ particles [16].

Here we report a novel solid state reaction method for fabricating nonstoichiometric LiFePO$_4$/C core–shell composites. This method has both advantages of carbon deposition method and liquid N$_2$ quenching measurements [16,17]. The samples acquired are composed of many microsphere-like core–shell particles and show high tap density. Meanwhile as the carbon shell is very thin (only 3–5 nm), it can benefit the Li$^+$ diffusion through the cathode/electrolyte interface. The nonstoichiometric composites of LiFePO$_4$ can also improve the electrochemical property as it may accelerate the diffusion of lithium ion in the particles as many papers reported [2,5,18]. Both Li$_{0.98}$Fe$_{1.01}$PO$_4$/C and Li$_{1.02}$Fe$_{0.99}$PO$_4$/C show good battery cyclability along with high tap density. We also compared electrochemical properties of the two different core–shell composites.

2. Experimental

2.1. Preparation of materials

The raw materials Li$_2$CO$_3$ (≥99.99 wt%), NH$_4$H$_2$PO$_4$ (≥99 wt%), and FeC$_2$O$_4$·2H$_2$O (≥99.81 wt%) were mixed at the appropriate ratios as Li$_{0.98}$Fe$_{1.01}$PO$_4$ and Li$_{1.02}$Fe$_{0.99}$PO$_4$ with planetary ball

---

* Corresponding authors. Fax: +86 25 8621 2844.
    E-mail addresses: yftang@nju.edu.cn (Y.F. Tang), yfchen@nju.edu.cn (Y. Chen).

milling for 24 h. Both precursors were finally dried at 60 °C. Two small disks with a certain amount of sucrose were used here as the carbon source to form the carbon shell in the vapor deposited process. Both precursors with the carbon source were first heated at 350 °C under purified N_2 gas flow for 5 h to decompose, then enclosed in two vacuumed quartz vessels respectively. The precursors in the vessels were sintered for 12 h at 700 °C. After this process, the two closed quartz vessels with samples were put into the liquid N_2 for quenching. Finally, the samples were acquired.

2.2. Measurements

The powders were characterized by X-ray diffraction (XRD, D/Max-RA, transmission electron microscopy (TEM, FEI Tecnai F20 S-Twins). For electrochemical measurements, a composite cathode was used. The cathode (8–10 milligram weight; Φ = 10 mm) was prepared by mixing the active materials with carbon black and PTFE in a weight ratio of 8:1:1 for electrochemical testing. The cells were assembled in Ar-filled glove box with the as-prepared cathode; a Li anode; a separator (Celgard polymer) saturated with a 1 mol L^{-1} $LiPF_6$ solution in ethylene carbonate and dimethyl carbonate (1:1, v/v). Charge–discharge experiments were performed in Land battery cycler over a voltage of 2.0–4.2 V (Land Instruments, China).

3. Results and discussion

Fig. 1 illustrates the preparation process and the possible mechanism as the formation of those core–shell composites. In our experiment, sucrose was used as the carbon source to form the carbon shell in the vapor deposited process which is quite different with the conventional measurements. Firstly, the precursors were heated at 350 °C for 5 h, then cooled to room temperature and filled in to the vessels under vacuum. When the vessels (which were heated at 700 °C for 12 h) were immersed into liquid N_2, the samples' temperature decreased rapidly and the gas-pressure in the tube declined. It caused the carbon vapor deposited onto the surface of the $Li_{0.98}Fe_{1.01}PO_4$ or $Li_{1.02}Fe_{0.99}PO_4$ particles and formed the thin carbon shell coated on $Li_{0.98}Fe_{1.01}PO_4$ and $Li_{1.02}Fe_{0.99}PO_4$ core. Finally, $Li_{0.98}Fe_{1.01}PO_4/C$ and $Li_{1.02}Fe_{0.99}PO_4/C$ composites as core–shell structure were acquired.
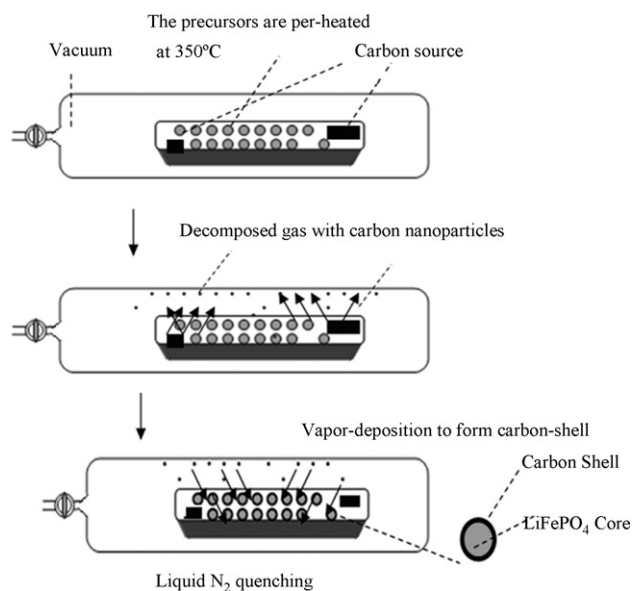

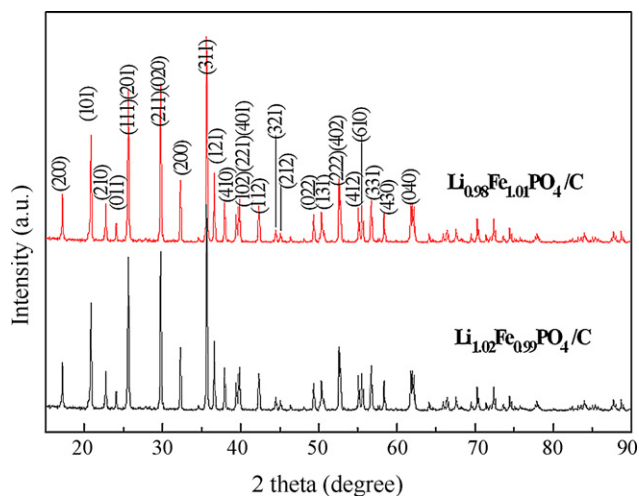**Fig. 1.** Mechanism of the formation of nonstoichiometric $LiFePO_4/C$ core–shell compositions.

Fig. 2. XRD patterns of $Li_{0.98}Fe_{1.01}PO_4/C$ and $Li_{1.02}Fe_{0.99}PO_4/C$.

Fig. 2 shows the XRD patterns of $Li_{0.98}Fe_{1.01}PO_4/C$ and $Li_{1.02}Fe_{0.99}PO_4/C$ core–shell composites with the standard pattern as olivine structure (JCPDS card no. 83-2092). Both samples can be well reflected by the typical structure of $LiFePO_4$ olivine phase. It is difficult to find any other impurity phase from the plots of both two samples which is ascribed to the quenching treatments [17]. The pure phase and high crystallinity as the samples guarantees good electrochemical performance which is approved hereinafter.

The morphologies of $Li_{0.98}Fe_{1.01}PO_4/C$ and $Li_{1.02}Fe_{0.99}PO_4/C$ core–shell particles were shown in Fig. 3. It can be seen from Fig. 3a and d that both of the samples were composed of many microparticles with some amorphous carbon contacted between them. The size of sphere-like particles is in the range of 100–200 nm. The high magnification pictures with corresponding crystal lattice stripes which are well confirmed with olivine $LiFePO_4$ were shown in Fig. 3b and d. It shows the continuous amorphous layer as the carbon shell coated on $Li_{0.98}Fe_{1.01}PO_4$ and $Li_{1.02}Fe_{0.99}PO_4$ core. Fig. 3c and f shows the HRTEM images of homogenous carbon shells where the thicknesses of the shells are 3–5 nm. These carbon shells can supply well electron conductivity which can improve the samples' electrochemical performance effectively [9–14]. They can also prohibit the oxidation of Fe^{2+} into Fe^{3+} and reduce the Fe^{3+} into Fe^{2+} which is a great problem for $LiFePO_4$ in the synthesis and preserve process, just like the carbon-thermal reduction method [19,20]. The tap density of $Li_{0.98}Fe_{1.01}PO_4/C$ core–shell sample is as high as 1.82 g cm^{-3}, whereas that of the $Li_{1.02}Fe_{0.99}PO_4/C$ core–shell sample is 1.77 g cm^{-3}. These high tap densities of the two samples (the commercial product is only about 1.00 g cm^{-3}, from Tianjin Sterlan-Energy Ltd., China) are because of the microsphere-like shape of the particles and ultrathin carbon shell.

Charge/discharge tests were conducted to evaluate the electrochemical performances of the two materials. Fig. 4a and b shows the profiles over the voltage of 2.0–4.2 V using charge–discharge galvanostatic cell with different specific currents, ranging from 0.2 C to 5 C. Both of the two samples have an excellent flat voltage plateaus. $Li_{1.02}Fe_{0.99}PO_4/C$ shows quite excellent rate performance (Fig. 4a). At the lowest discharge rate of 0.2 C (5 h charge and 5 h discharge), the voltage profile dropped rapidly to end-discharge voltage after flat voltage plateau and the whole discharge capacity is 164 mAh g^{-1}. The discharge capacities at other current rates are 161 mAh g^{-1} (0.5 C); 156 mAh g^{-1} (1 C); 151 mAh g^{-1} (2 C) and even at the current rate higher as 5 C, a capacity of 145 mAh g^{-1} is still obtained. This excellent rate performance is mainly ascribed to the quite stable crystal structure of the $LiFePO_4$ phase and good electron conductivity supplied by the thin carbon shell. The $Li_{0.98}Fe_{1.01}PO_4/C$
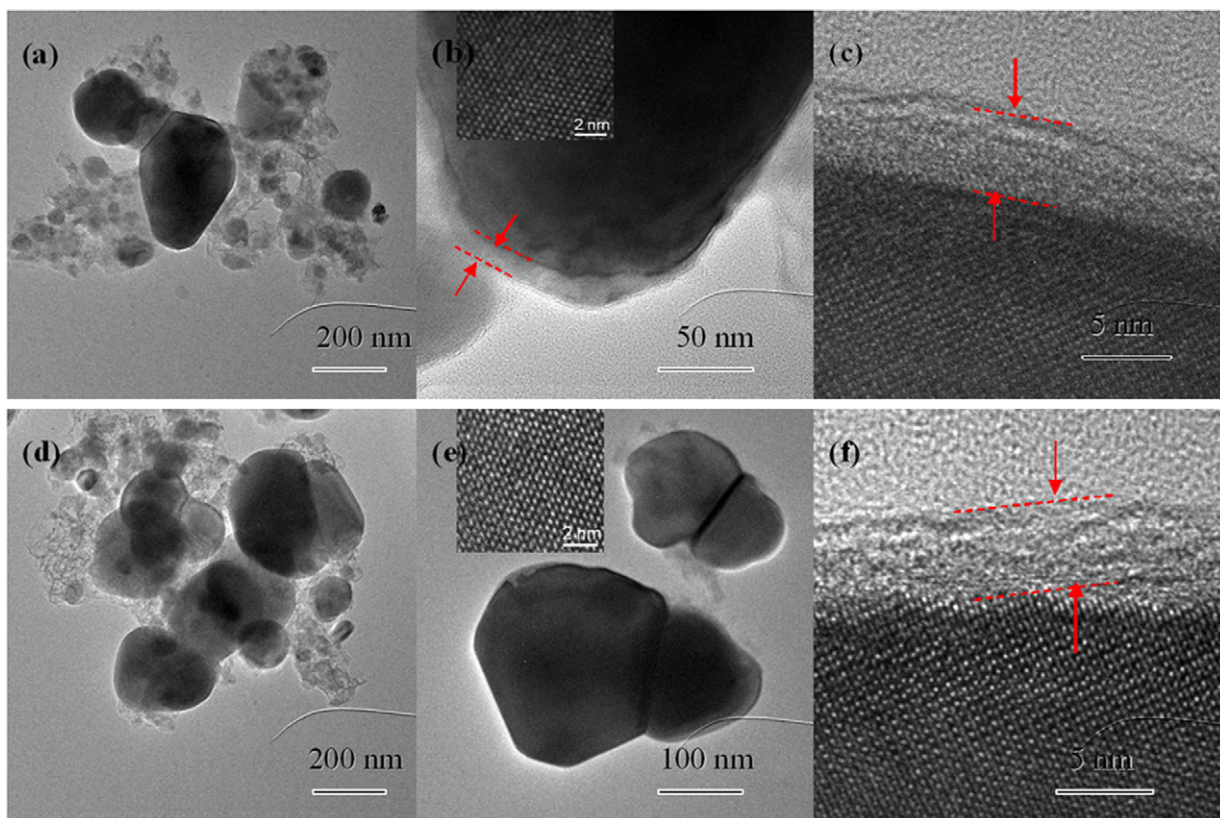
Fig. 3. TEM of $Li_{0.98}Fe_{1.01}PO_4$/C and $Li_{1.02}Fe_{0.99}PO_4$/C core–shell particles. (a and d) The morphology of (a) $Li_{0.98}Fe_{1.01}PO_4$/C and (d) $Li_{0.98}Fe_{1.01}PO_4$/C. (b and e) HRTEM of (b) $Li_{0.98}Fe_{1.01}PO_4$/C and (e) $Li_{0.98}Fe_{1.01}PO_4$/C with corresponding crystal lattice stripes. (c and f) The carbon shell on the surface of (c) $Li_{0.98}Fe_{1.01}PO_4$/C and (f) $Li_{0.98}Fe_{1.01}PO_4$/C.

core–shell sample shows relatively poor rate capability, just as 145 mAh g^{-1} at 0.2 C; 143 mAh g^{-1} at 0.5 C; 136 mAh g^{-1} at 1 C; 134 mAh g^{-1} at 2 C and 116 mAh g^{-1} at 5 C. The weakness of the electrochemical performance as $Li_{0.98}Fe_{1.01}PO_4$/C core–shell sample can be attributed to more Fe–Li (center dot) defects in Fe excessive sample which block the diffusion of lithium along the corresponding channel [18].

Cycle stabilities of $Li_{0.98}Fe_{1.01}PO_4$/C core–shell sample and $Li_{1.02}Fe_{0.99}PO_4$/C core–shell sample with various discharge current rates are demonstrated in Fig. 5a. We tested the batteries at varied current rates: 0.2 C for 5 cycles; 0.5 C for 5 cycles, 1 C for 5 cycles, 2 C for 5 cycles, 5 C for 5 cycles, repeat 0.2 C for 5 cycles, respectively. At

first, the capacity of both core–shell composites increases slightly, corresponding to the battery activation process. It can be seen the discharge capacity of both samples are very stable at each current rate. As the current rates raised step by step, the discharge capacities of the sample decreased slightly. The signal is that when the current rate reverses to 0.2 C after 5 C rate discharge, both samples increased to high capacities which are equal or more than the original value. This indicates that both samples can be tolerant to varied charge and discharge current. It is the desirable characteristic required for the high power application [21]. The cycling characteristics of both samples at 0.2 C and 5 C were also given in Fig. 5b. Both samples show superior cycle stability with excellent
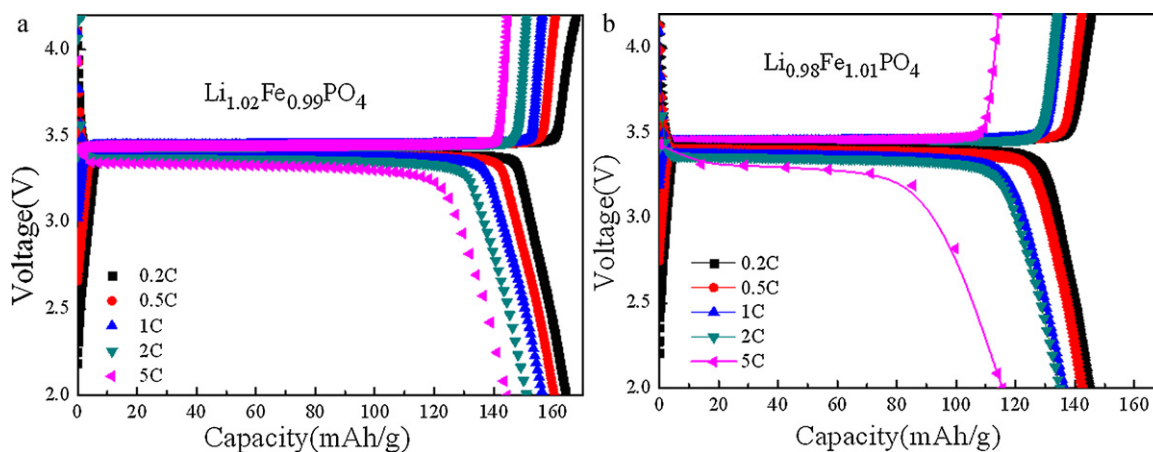

Fig. 4. Charge/discharge curves of $Li_{0.98}Fe_{1.01}PO_4$/C and $Li_{1.02}Fe_{0.99}PO_4$/C with different specific currents ranging from 0.2 C to 5 C. (a) Charge/discharge plots of $Li_{1.02}Fe_{0.99}PO_4$/C. (a) Charge/discharge plots of $Li_{0.98}Fe_{1.01}PO_4$/C.
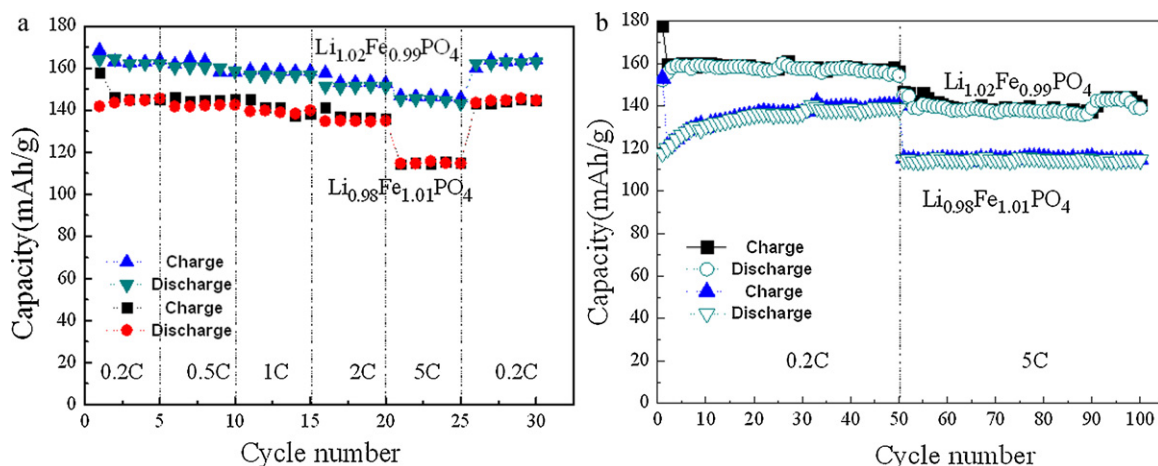
Fig. 5. Cycle performance of $Li_{0.98}Fe_{1.01}PO_4/C$ and $Li_{1.02}Fe_{0.99}PO_4/C$. (a) Cycle stabilities of $Li_{0.98}Fe_{1.01}PO_4/C$ core–shell sample and $Li_{1.02}Fe_{0.99}PO_4/C$. (b) Cycling characteristics of $Li_{0.98}Fe_{1.01}PO_4/C$ and $Li_{1.02}Fe_{0.99}PO_4/C$ at 0.2 C and 5 C.

coulombic efficiency almost 100% in the whole process whatever at high or low current rates. All of these set out by Fig. 5a and b can be ascribed to the good electro-conductivity supplied by well coated thin carbon shell and high crystal structure stability as the well crystalline samples.

4. Conclusions

In conclusion, we synthesized the nonstoichiometric $Li_{0.98}Fe_{1.01}PO_4/C$ and $Li_{1.02}Fe_{0.99}PO_4/C$ core–shell composites with high tap density were synthesized by a novel method. We found that both samples show sphere-like morphology coated with the homogenous carbon shells (3–5 nm) and reveal outstanding coulombic efficiency, good cycle stabilities which can meet the demands of high power applications. Moreover, we found $Li_{1.02}Fe_{0.99}PO_4/C$ core–shell composite is obviously better than $Li_{0.98}Fe_{1.01}PO_4/C$.

Acknowledgements

References

[1] K. Green, J.C. Wilson, Electron. Commun. Eng. J. 13 (2001) 43–47.
[2] S.Y. Chung, J.T. Bloking, Y.M. Chiang, Nat. Mater. 1 (2002) 123–128.
[3] C. Delacourt, P. Poizot, J.M. Tarascon, C. Masquelier, Nat. Mater. 4 (2005) 254–260.
[4] C. Delmas, M. Maccario, L. Croguennec, F. Le Cras, F. Weill, Nat. Mater. 7 (2008) 665–671.
[5] B. Kang, G. Ceder, Nature 458 (2009) 190–193.
[6] P.S. Herle, B. Ellis, N. Coombs, L.F. Nazar, Nat. Mater. 3 (2004) 147–152.
[7] S.W. Oh, S.T. Myung, S.M. Oh, C.S. Yoon, K. Amine, Y.K. Sun, Electrochim. Acta 55 (2010) 1193–1199.
[8] M.E. Zhong, Z.T. Zhou, Mater. Chem. Phys. 119 (2010) 428–431.
[9] Y.G. Wang, Y.R. Wang, E.J. Hosono, K.X. Wang, H.S. Zhou, Angew. Chem. Int. Ed. 47 (2008) 7461–7465.
[10] M.M. Ren, Z. Zhou, X.P. Gao, W.X. Peng, J.P. Wei, J. Phys. Chem. C 112 (2008) 5689–5693.
[11] Y. Zhang, C.S. Sun, Z. Zhou, Electrochem. Commun. 11 (2009) 1183–1186.
[12] B. Zhao, Y. Jiang, H.J. Zhang, H.H. Tao, M.Y. Zhong, Z. Jiao, J. Power Source 189 (2009) 462–466.
[13] H.M. Xie, R.S. Wang, J.R. Ying, L.Y. Zhang, A.F. Jalbout, H.Y. Yu, G.L. Yang, X.M. Pan, Z.M. Su, Adv. Mater. 18 (2006) 2609–2613.
[14] Y.L. Cao, L.H. Yu, T. Li, X.P. Ai, H.X. Yang, J. Power Source 172 (2007) 913–918.
[15] W.X. Peng, L.F. Jiao, H.Y. Gao, Z. Qi, Q.H. Wang, H.M. Du, Y.C. Si, Y.J. Wang, H.T. Yuan, J. Power Source 196 (2011) 2841–2847.
[16] I. Belharouak, C. Johnson, K. Amine, Electrochem. Commun. 7 (2005) 983–988.
[17] X.G. Gao, G.R. Hu, Z.D. Peng, K. Du, Electrochim. Acta 54 (2009) 4777–4782.
[18] P. Axmann, C. Stinner, M. Wohlfahrt-Mehrens, A. Mauger, F. Gendron, C.M. Julien, Chem. Mater. 21 (2009) 1636–1644.
[19] M. Cuisinier, J.F. Martin, N. Dupre, A. Yamada, R. Kanno, D. Guyomard, Electrochem. Commun. 12 (2010) 238–241.
[20] X. Xia, Z.X. Wang, L.Q. Chen, Electrochem. Commun. 10 (2008) 1442–1444.
[21] G.X. Wang, H. Liu, J.A. Liu, S.Z. Qiao, G.Q.M. Lu, P. Munroe, H. Ahn, Adv. Mater. 22 (2010) 4944–4948.